TO: W. Anderson   TAMM 6115-22
          D 578, Z-1   13 April 1966
          Rocketdyne, Canoga

FROM: E. Jackson
          D 596-115, Z-4
          Rocketdyne, Canoga

SUBJECT: Quarterly Progress Report for Period 1 January 1966 through
          31 March 1966, Pump Discharge Oscillation Study

SUMMARY

Progress achieved during the third quarter of study on the Pump
Discharge Oscillation contract is presented along with a schedule
for completing the remaining work on the contract. In the acoustic
wave transmission study the impedance equations of curved elbows,
orifices, and straight pipes were derived which completes the study
of wave transmission in elements. The test program for both the
acoustic wave transmission and generation was planned and very
recently initiated. The hot-wire anemometer purchased for this
test program appears to be working. A computer program was written
for computing the unsteady blade loading due to the passage of
viscous wakes. The derivation of the conditions for wave rein-
forcement in pumps with a multi-vaned diffuser is presented, and
a test program for confirming these analytical results is planned
for the Mark 26 fuel pump in the J-2 Air Rig.

Author

E. Jackson

E. Jackson
Responsible Engineer
Pump Discharge Oscillation Contract

EJ:br

Approved:

K. Rothe
Chief
Turbomachinery Specialties

BLADE WAKE OSCILLATIONS

ACOUSTIC WAVE GENERATION

In the study of the generation of acoustic waves by the flow leaving the impeller, attention has been primarily focused on the unsteady pressure distribution on stationary blades downstream of the impeller. In the last quarterly report four effects which cause unsteady blade loading were distinguished and each discussed in general terms. The effect assumed to be most significant is the viscous wake effect. The analytical procedures which had been developed for studying this wake effect have been programmed on the digital computer to permit numerical calculation of the unsteady pressures due to this effect. This computer program and its results are discussed below. A decision has been made not to attempt to program on the computer the other three effects. A further discussion of these three effects and a discussion of the decision to not program each is to be written but is not complete enough to be included in this report. However, one significant factor influencing this decision is the hypothesis that the acoustic waves of interest are generated by the velocity boundary condition at the volute tongue cross-section and not by the tongue loading. Experimental data is required for further verification of this hypothesis.

Wake Effect

The wake effect considers the unsteady forces on a downstream blade passing through the viscous wakes of an upstream system of blades. These viscous wakes are formed as the boundary layer fluid along the surfaces of the upstream blade leaves this blade. The wakes represent a region of velocity defect with respect to the blades that shed them, but to a downstream blade row in relative motion to the wakes they represent jets of fluid. These wakes, in general, contain velocity components both parallel and perpendicular to the downstream blades. Only the perpendicular component is of interest in the following calculations of blade loading effects.

Since this downstream blade row is passing through these viscous wakes, the wakes appear as a periodic unsteady flow. To determine the effects of this unsteady flow field on the blades, the theory of single thin airfoils in non-uniform motion is applied. The basic assumptions upon which the theory is built are:

1) the fluid is inviscid and incompressible
2) each blade row can be represented by an infinite, <u>two-dimensional</u> cascade of airfoils
3) the airfoils are thin, slightly cambered, and have small turning angles
4) the flow about the airfoil can be represented at any instant by a vortex sheet superimposed upon a mean flow
5) all unsteady velocity components are small compared to the mean velocity, and their effects can be linearly superimposed on the "stationary" or other unsteady effects, and
6) the velocity at the trailing edge of the airfoil is zero.

Assumption #1 regarding the inviscid character of the fluid does not prevent the analysis of the effects of the viscous wakes described above. The wake characteristics must be determined using viscous flow theory. However, once the wake is described, its effect on the downstream blades can be determined from potential theory.

Due to assumption #6, each airfoil creates a circulation about itself. However, any change in the circulation about the airfoil is accompanied by the shedding of vorticity such that the total circulation in the system is always zero. This vorticity shed by the blade moves with the fluid (in contrast with the airfoil which moves relative to the fluid). Therefore, an unsteady flow field creates an unsteady circulation about the airfoil which is accompanied by a wake of vorticity trailing the airfoil. The pressure or velocity induced on the airfoil by this unsteady flow is calculated under these assumptions by computing the quasi-steady effects of the incoming flow field plus the integrated effects of the vorticity wake trailing the airfoil.

Von Karman and Sears[1]* review these fundamental concepts and associated equations of the circulation theory of airfoils. They then proceed to derive the equations for the lift and moment on the airfoil due to an unsteady flow. The equations they derive and the approach they follow are the basis for computing the unsteady blade loading due to both the wake effect[2] and the circulation effect [3] as considered by Kemp and Sears. However, in none of these papers is the actual blade unsteady pressure and velocity distribution derived, all emphasis being placed on the lift and moment. Meyer [4] using the same approach does compute the unsteady pressure (and velocity) distribution for the case of a sinusoidal viscous wake profile, and he shows that this pressure integrated over the blade length agrees with the lift of Kemp and Sears. This result of Meyer is sufficient for computing the pressures due to any other viscous wake profile since the profile can be represented by a Fourier sine series and each term considered separately then linearly superimposed. However, there is a simpler approach presented by Lefcort which was used here.

After Meyer derived the pressure distribution for the sinusoidal viscous wake profile, he proceeded to derive the pressure distribution for an arbitrary wake profile of infinitely thin width, i.e. the wake width to blade chord ratio is extremely small. In such a case the pressure gradient is given by Meyer as

$$\frac{\partial p}{\partial x} = \pm 2\rho\frac{VW}{c^2} \frac{T(t')}{(1 + x')(1 - x'^2)^{1/2}} \qquad (1)$$

where

$p = p(x, t) = $ pressure
$x = $ distance along the blade chord from the centerline of the chord
$\rho = $ fluid density
$V = $ mean (steady) fluid velocity
$c = $ blade chord
$x' = 2x/c = $ dimensionless distance
$b = $ wake half-width
$w(\xi) = $ the viscous wake velocity component perpendicular to the blade
$t = $ time
$t' = 2Vt/c = $ dimensionless time

---

* Numbers in parentheses refer to references at the end of the report.

and where

$$W = \int_{-b}^{b} w(\xi)\, d\xi \tag{2}$$

and

$$T(t') = \frac{1}{\pi} \int_{-\infty}^{\infty} S(w)\, e^{iwt'}\, dw \tag{3}$$

where $S(w)$ is the Sears' Function. This Sears' Function is defined as

$$S(w) = \left\{ iw\left[K_0(iw) + K_1(iw) \right] \right\}^{-1} \tag{4}$$

where K_0 and K_1 are modified Bessel functions of the second kind. The upper and lower signs of eq. (1) refer to the suction and pressure side respectively.

Lefcort, setting $x' = \cos\Theta$, integrated eq. (1) to yield the pressure,

$$p(\Theta, t') = \mp \rho V\, \overline{W} T(t')\, \tan\frac{\Theta}{2} \tag{5}$$

where Lefcort's $\overline{W}$ is given by W/c. Lefcort then assumes that any velocity profile of a viscous wake can be divided into a finite number of increments such that each increment has a small width. These increments can then be treated separately using eq. (5), and the results superimposed. Or, as shown by Lefcort, the superposition can be defined by a single integral equation such that

$$p(x', t_0') = \mp \rho V\tilde{W}(t_0')\, \tan\Theta/2 \tag{6}$$

where

$$\tilde{W}(t_0') = -\frac{1}{2} \int_{-\infty}^{\infty} k_2(t_0' + \xi')\, \frac{dw(\epsilon')}{d\xi'}\, d\xi' \tag{7}$$

$$k_2(t') = \int_{-1}^{t'} T(t')\, dt' \tag{8}$$

$$\xi' = 2\xi/c$$

and t_0' is the dimensionless distance obtained by dividing the distance between the viscous wake centerline and the blade chord centerline by one-half the chord length. (These steps and definitions are not elaborated on here since they are presented in detail and with clarity in the referenced papers.) If the viscous wake velocity profile, $w(\xi)$, is known, eqs. (6) and (7) can be solved to determine the unsteady pressure distribution.

A digital computer program was written to numerically solve eqs. (6) and (7). The function, k_2, is a complex function of modified Bessel functions such that it is most easily represented on the computer by dividing the function over a number of ranges and curve fitting each range by a polynomial. A set of nine second order polynomials was found to adequately match the tabulated values of $k_2(t')$ as given by Lefcort. Solution of eq. (7) also

requires the first spatial derivative of the wake velocity. To permit analysis of arbitrary wake profiles, the velocity derivative $dw(\xi)/d\xi$ is assumed to be expressible by four functions, each defined over a given quadrant of the total wake width. No restrictions are placed on the four functions except that each is a function of only one independent variable, ξ. Therefore, any wake profile, whose quadrants can be independently curve fit, can be handled by the computer program. All profiles of practical interest will be of finite width (e.g. 2b in Meyer's notation) such that the integral in eq. (7) will assume finite limits of integration (e.g., from -b to b, using again Meyer's notation). The general approach followed in the program is then:

1) Choose a position of the wake relative to the blade, i.e. choose a value of t_o'.

2) Numerically integrate eq. (7) to determine $\widetilde{W}(t_o')$ using Simpson's rule.

3) Using eq. (6) and the relationship, $x' = \cos\Theta$, compute the pressure at distributed points along the blade due to this wake position.

4) Increment t_o' to get a new wake position and repeat steps 1) through 4).

Due to the behavior of k_2 it is easily seen that the wake does not effect the blade until the leading edge of the wake reaches the leading edge of the blade. This determines the initial value of t_o'. Initially small changes in t_o' result in rapid pressure changes such that the incremental changes in t_o' should be small. In the program the initial increments were one-tenth of the dimensionless wake width. After the wake trailing edge is past the leading edge of the blade the increments were increased to one wake width.

Some sample results obtained from the program are shown in Figs. 1, 2, and 3. In Fig. 1 the computer program results are compared with Lefcort's theoretical results. The wake profile and other pertinent parameters are given by Lefcort. The pressure shown is at Lefcort's transducer location #1, and his theoretical curve was read from his Fig. 14 (a). The agreement is good considering the inaccuracies in reading Lefcort's curve from the figure. The comparison of the experimental with the theoretical is given also by Lefcort and indicates the theoretical results to be accurate enough for present applications.

In Fig. 2 the effect of the wake width is illustrated by comparing the loading for identical wake velocity profiles with variable wake half-width to blade chord length ratios. As the relative wake width decreases the pressure amplitude is reduced, and the effect of the wake is concentrated on a much smaller extent of the blade.

In Fig. 3 the effect of the wake profile is shown by comparing a triangular wake with the more classic wake profile given as $w(\xi) = \cos^2(\pi\xi/2B)$. Each wake has the same maximum amplitude which has been normalized to a value of 1.0, and each has the same integrated velocity defect. The results are similar, the differences being less than the differences encountered in the comparison of experimental and theoretical results.
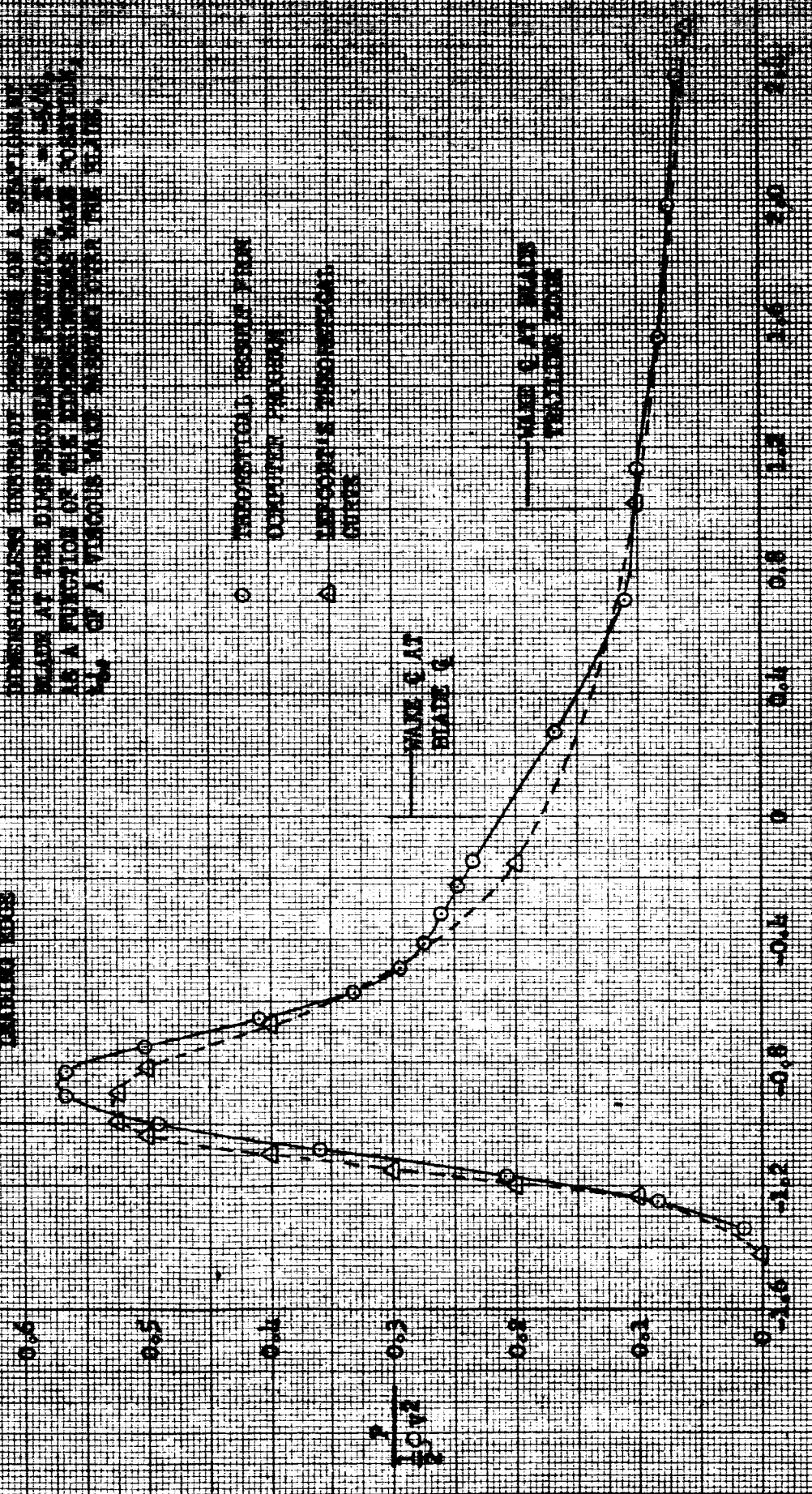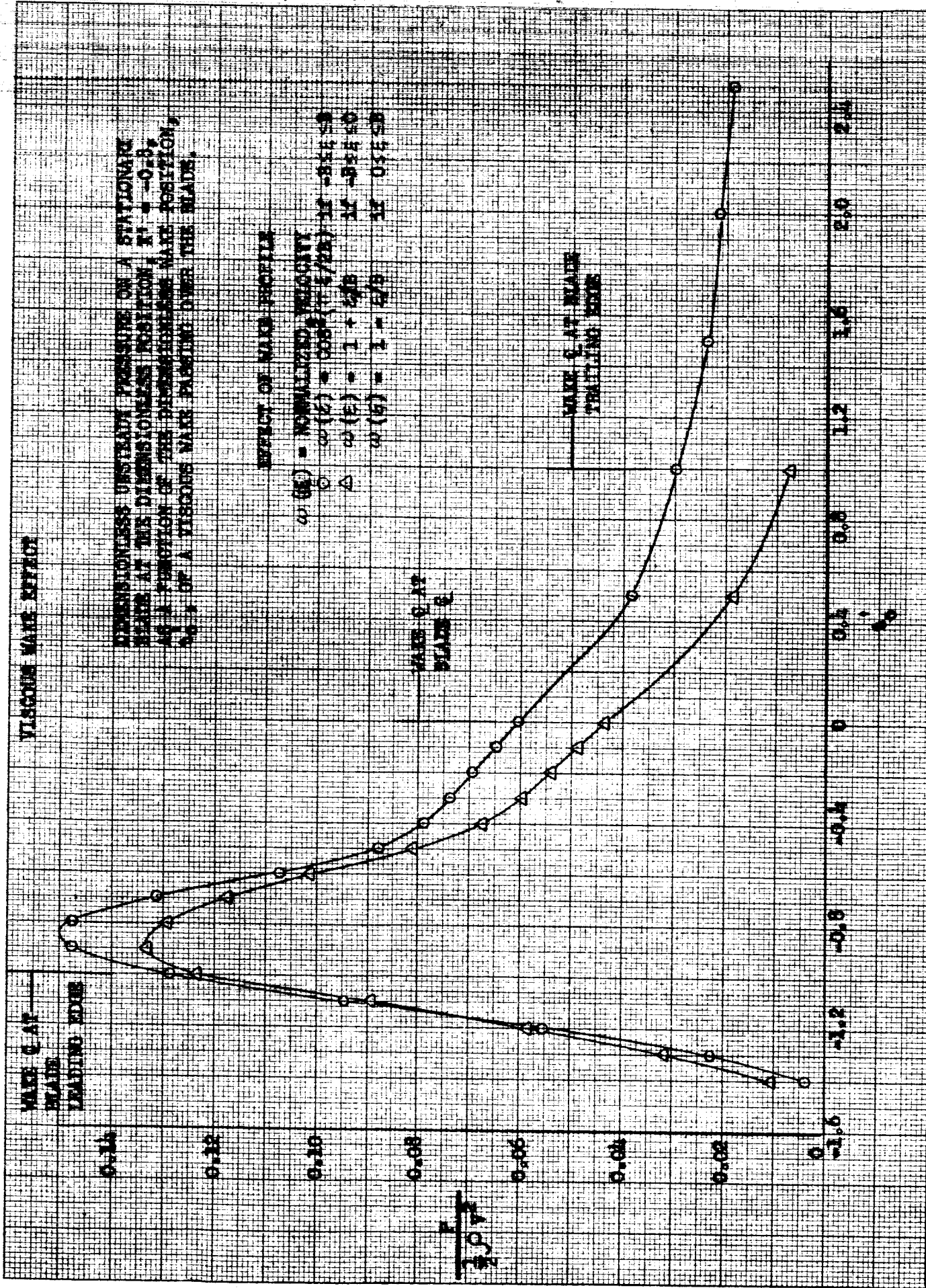
FIG. 1.
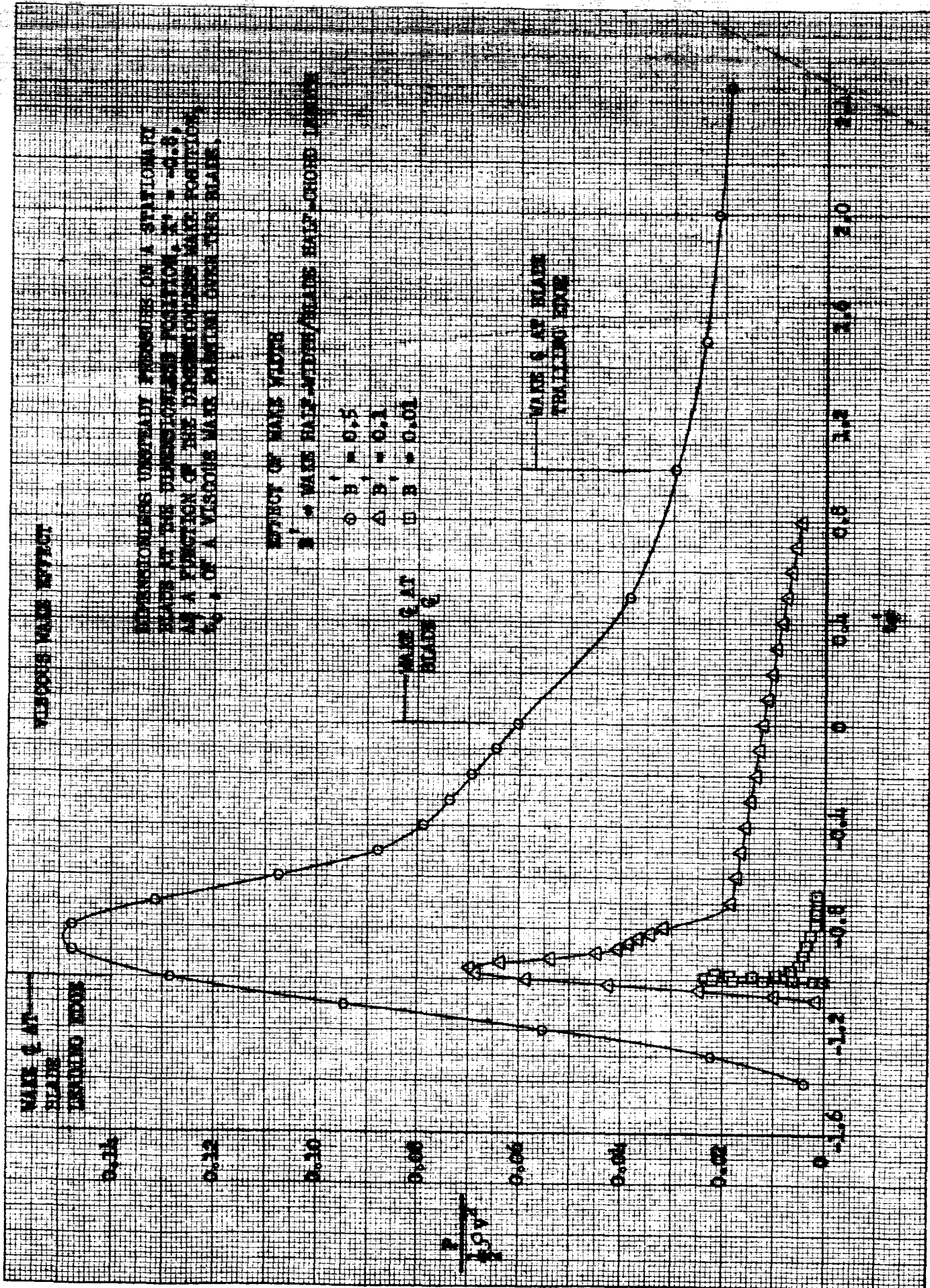
FIG. 2.

ACOUSTIC WAVE TRANSMISSION

Wave Transmission Around An Elbow

During the past quarter, digital computer programs were completed for computing the impedance of a curved elbow with arbitrary radius ratio and arbitrary angle. The approach taken for the solution is identical to that used for the kinked, or mitered, elbow, and again a two-dimensional elbow is assumed to permit the analysis. A sketch of the general curved elbow is shown below indicating the significant variables.
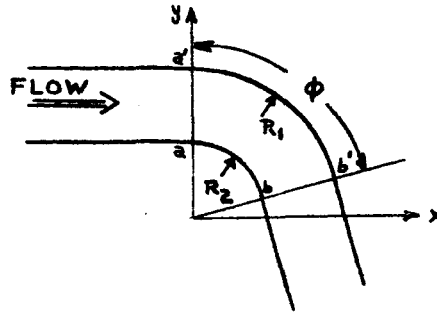
The first step, of course, is to define the velocity profile at the entrance and exit of the elbow, i.e. along a - a' and b- b', respectively. This velocity was determined on the computer by solution of the Laplace equation representing two-dimensional steady potential flow. The solution was accomplished using the familiar finite difference equations which were solved by iterative techniques until convergence was reached.

For the kinked elbows the velocity profile was curve fit, and then the impedance computed. For the curved elbows, the velocity is a function of both R_2/R_1 and ϕ (as defined in the previous sketch) and a curve fit equation which would be capable of handling a wide range of these two variables would be very complicated and much less accurate than was the case with the kinked elbow. As a result, the velocity profile obtained from the computer program was plotted on a large scale and a "smooth" curve drawn through the points by eye. From this curve the velocity (U_j) at many more points (ξ_j) were read, and these values of velocity were then input into the computer in the impedance program.

The equations for computing the impedance are determined by following the same steps given in detail in the first quarterly report. To compute the impedance integrals of the form

$$I = \int_0^{1.0} U(\xi) \cos \pi m \xi \, d\xi , \qquad (9)$$

where

$$\xi = \frac{y - R_2}{R_1 - R_2} \qquad (10)$$

and $U(\xi)$ is the velocity along $a - a'$ in the x direction, must be solved for increasing values of m until m is sufficiently large to result in a converged value of the impedance. At the points $\xi = \xi_i$, $i = 1, 2, \ldots, N$ the values U_i are stored in the computer. It is now assumed that

$$\text{if } \xi_{i-1} \le \xi \le \xi_i \quad , \quad U(\xi) = C_i + D_i \xi \tag{11}$$

That is, between the discrete values of ξ read into the computer the velocity is approximated by a linear segment. The error in this approximation is expected to be insignificant. Using eq. (11), eq. (9) can be solved as follows:

$$I = \sum_{i=2}^{N} \int_{\xi_{i-1}}^{\xi_i} \left[C_i + D_i \xi \right] \cos \pi m \xi \, d\xi \quad . \tag{12}$$

This equation can be readily integrated such that numerical integration procedures are not required. This approach was much more efficient on the computer than the approach consisting of a single curve fit expression for the velocity because of the difficulties of integrating exactly an equation of the form of eq. (9) when $U(\xi)$ assumes various forms.

The impedance results obtained are shown in Figs. 4, 5, and 6 for $= 90, 60,$ and 30 degrees, respectively and for $R_o/R_1 = 0.01, 0.1, 0.2,$ and 0.5 for each ϕ. If the impedance for $R_o/R_1 = 0.01$ is compared with the impedance of the kinked elbow shown as Fig. 2 in the last quarterly report, it will be seen that the two are approximately equal. That is, the fact that the outer wall is curved seems to have essentially no effect on this theoretical impedance.

Wave Transmission Past Orifices

The impedance of orifices has been the subject of previous investigations which are reported in the literature. The classical impedance of a circular orifice is given as

$$Z = \frac{\rho c k^2}{2\pi} + i \frac{\rho l' w}{\pi a^2} \tag{13}$$

where

$$
\begin{aligned}
l' &= 1 + 1.7a & \tag{14}\\
a &= \text{orifice radius} \\
1 &= \text{orifice length} \\
\rho &= \text{fluid density} \\
c &= \text{fluid acoustic velocity} \\
w &= \text{circular frequency} \\
k &= w/c
\end{aligned}
$$

This impedance contains a radiation resistance term ($= \rho c k^2/2\pi$) which is usually small and a mass reactance ($= \rho l' w/\pi a^2$) containing both the mass within the orifice length and an end correction term variously reported as $(1.7a)$ or $(16a/3\pi)$. Actually, eqs. (13) and (14) give the impedance of a circular orifice in an infinite wall when the orifice dimensions ("a" and "l") are small compared to the wavelength of the sound. In addition, the validity of eq. (13) is based on the assumption that the viscosity is small, and the velocity of flow through the orifice is sufficiently small for laminar flow to exist. The assumption of small orifice dimensions relative to the wave length is maintained throughout the literature, however the relaxing of the

IMPEDANCE OF A 2-DIMENSIONAL CURVED ELBOW

ϕ = 90 DEGREES

$R_2/R_1 = 0.01$
" = 0.10
" = 0.20
" = 0.50

R_2, R_1 = INNER AND OUTER ELBOW RADIUS
ϕ = TURNING ANGLE OF ELBOW
z_e = ELBOW IMPEDANCE
$\rho_0 c/S$ = ACOUSTIC IMPEDANCE OF MEDIUM
$K = 2\pi f/c = 2\pi/\lambda = 2\pi$ (WAVELENGTH)$^{-1}$

$\frac{z_e}{\rho_0 c/S}$

DIMENSIONLESS FREQUENCY = $K(R_1 - R_2)$

FIG. 4.

IMPEDANCE OF A 2-DIMENSIONAL CURVED ELBOW

$\phi = 60$ DEGREES

$R_2/R_1 = 0.01$
$" = 0.10$
$" = 0.20$
$" = 0.50$

$R_2, R_1 = $ INNER AND OUTER ELBOW RADIUS
$\phi = $ TURNING ANGLE OF ELBOW
$Z_w = $ ELBOW IMPEDANCE
$\rho c/S = $ ACOUSTIC IMPEDANCE OF MEDIUM $\to 1.0$
$K = 2\pi f/c = 2\pi/\lambda = 2\pi \times (\text{WAVELENGTH}^{-1})$

$\dfrac{Z_w}{\rho c/S}$

5.0
4.0
3.0
2.0
1.0
0

0.4   0.8   1.2   1.6   2.0   2.4   2.8   3.2

DIMENSIONLESS FREQUENCY = $K(R_1 - R_2)$

FIG. 5.

IMPEDANCE OF A 2-DIMENSIONAL CURVED ELBOW

φ = 30 DEGREES

$R_2/R_1 = 0.01$
" = 0.10
" = 0.20
" = 0.50

R_2, R_1 = INNER AND OUTER ELBOW RADIUS
φ = TURNING ANGLE OF BEND
Z_e = ELBOW IMPEDANCE
$\rho c/S$ = ACOUSTIC IMPEDANCE OF MEDIUM
k = $2\pi f/c = 2\pi/\lambda$ (DIMENSIONAL)

$\frac{Z_e}{\rho c/S}$

DIMENSIONLESS FREQUENCY = $k(R_1 - R_2)$

0   0.4   0.8   1.2   1.6   2.0   2.4   2.8   3.2

1.0   2.0   3.0   4.0

FIG. 6.

other assumptions has been investigated, and correcting terms have been derived either analytically or experimentally.

If the viscosity of the medium is significant, and the heat conductivity can be neglected, Sivian (6) gives the impedance of the circular orifice as

$$Z = \frac{1'}{\pi a^2} \, i \rho w \, \frac{1.0}{1.0 - \dfrac{2.0}{\Theta a(-2i)^{1/2}} \dfrac{J_1(\Theta a(-2i)^{1/2})}{J_0(\Theta a(-2i)^{1/2})}} \tag{15}$$

where

$$\Theta = (w \rho /2\mu)^{1/2} \tag{16}$$

and μ is the coefficient of viscosity. Sivian has neglected the radiation resistance in this case. If $\mu = 0.0$, then Θ is infinite, and eq. (15) simplifies to give the imaginary part of eq. (13). If

$$a > 10 \sqrt{\frac{\mu}{2 \pi \rho f}} \tag{17}$$

where $f \, (= w/2\pi)$ is the oscillation frequency, then Kinsler and Frey (7) show that eq. (15) can be simplified to give a term

$$R_v = \frac{\sqrt{2 \mu \rho w}}{\pi a^3} \, 1' \tag{18}$$

which should be added to both the resistance and reactance of eq. (13). For air at room temperature eq. (17) yields

$$a > \frac{0.61}{\sqrt{f}} \text{ inch}$$

or, if $f \geq 100$ cps, then $a > 0.06$ inches which is generally observed.

Both Sivian and Kinsler and Frey show that the heat conductivity can be included by using an effective viscosity in either eq. (16) or (18), respectively. If the walls are good heat conductors in comparison with the flowing medium, then this effective viscosity should be used. Letting μ' be the effective viscosity, Sivian gives

$$\mu' = \mu \left[1.0 + (\gamma - 1)(\sqrt{1.0/Pr}) \right]^2 \tag{19}$$

while Kinsler and Frey give

$$\mu' = \mu \left[1.0 + (\gamma - 1)(1.0/Pr)(1.0/\sqrt{\gamma}) \right]^2 \tag{20}$$

where γ = specific heat ratio and Pr is the Prandtl number. For air, $\gamma \simeq 1.41$ and $Pr \simeq 0.73$ such that both eq. (19) and (20) yield $\mu' \simeq 2.2\mu$.

Probably more important in the present fields of application is the effect of the velocity of flow on the orifice impedance. These changes of impedance with velocity are attributed to flow circulations and turbulence and could result from either an increased intensity of the incident oscillations or a steady turbulent flow upon which the oscillating flow is superimposed. An increasing velocity will increase the resistance and decrease the reactance term of the impedance.

Sivian estimated the effect of the kinetic energy of the medium in the orifice on the orifice resistance and found that a resistance term of amplitude

$$R_F = 1/2 \; \rho \frac{U}{\pi a^2}$$

(21)

must be added to the resistance due to radiation and viscosity. In general, eq. (21) underestimated the effect of velocity. Utvik et al[8] derived a theoretical resistance which in the units of this paper is given by

$$R_F = \frac{3}{2} \; \rho \frac{U}{\pi a^2}$$

(22)

which is three times larger than used by Sivian. However, these same authors point out that the value in eq. (22) is derived under ideal conditions and that actually a flow coefficient, K_f, should be used such that

$$R_F = \frac{3}{2} \; \rho \; K_F \frac{U}{\pi a}2$$

(23)

In a comparison with experimental data a value of K_f of 0.5 was used, and good agreement was obtained.

Less information is available on the velocity effects on reactance than on resistance. Utivk et al (8) indicate that for thin orifices, i.e. $1 < 2a$, the acoustic reactance begins to decrease at a critical velocity of

$$U_{cr} = 2 \pi f l$$

(24)

and continues until a minimum reactance is reached when fully developed turbulent flow is reached which is assumed to occur at a Reynolds number of 2000, or at a velocity of

$$U_T = \frac{2000 \; \mu}{2 \, a \, \rho}$$

(25)

The minimum reactance is given as three-eighths of the low velocity reactance.

Another significant influence on the reactance is the wall effect when the orifice exists in a tube. If the tube radius is "r" and "a" is again the orifice radius, then Bolt et al (9) show that the classical low velocity reactance given in eq. (13) should include a correction factor δ such that

$$X = \frac{w \rho}{\pi a^2} (1 + 1.7 \delta a) \qquad (26)$$

where although δ is actually a rather complicated function of both a/r and rf/c, it can be conveniently approximated as

$$\delta = 1.0 - (a/r). \qquad (27)$$

Bolt et al give a further empirical correction for the case where the radius of the orifice is less than one centimeter. This correction involves replacing "a" in eq. (26) with "a'" where

$$a' = a \left\{ 0.245 \left[3 + (a)^{1/2} \right] \right\}^{1/3}. \qquad (28)$$

In the event of an orifice plate with multiple orifices the effective tube radius "r" to be used in eq. (27) might be determined by the relative distance between holes with a resulting reduction in the reactance term.

In conclusion, the orifice resistance is seen to consist of a radiation term, viscosity term with a correction for heat conductivity, and a velocity term. The reactance term is formed from the classical mass expression with a correction for both velocity and wall interaction effects.

Wave Transmission In Straight Ducts

The transmission of waves in straight pipes is well known, exact solutions having been obtained for both the non-viscous "waterhammer" equations and the viscous equations under certain simplifying assumptions including the assumption of laminar flow. However, for the convenience of the reader the derivation of the solution to the non-viscous equations is presented here, the final solution being expressed in terms of the time delay operators. These equation forms will be used in analog computer models of the ducting in the systems to be studied in this study program.

Consider the linear, one-dimensional wave equation

$$\frac{\partial^2 \psi}{\partial x^2} - \frac{1}{c^2} \frac{\partial^2 \psi}{\partial t^2} = 0 \qquad (29)$$

where ψ is the velocity potential such that the velocity and pressure are respectively defined as

$$v = - \frac{\partial \psi}{\partial x} , \qquad (30)$$

$$p = \rho \frac{\partial \psi}{\partial t} . \qquad (31)$$

The general solution of eq. (29) is

$$\Psi = Ae^{iw(\frac{x}{c} + t)} + Be^{iw(\frac{x}{c} - t)} \tag{32}$$

where A and B are constants representing the amplitude of an incident and reflected wave system in the pipe. Substituting eq. (32) into eqs. (30) and (31) yields

$$v(x,t) = -i \frac{w}{c} e^{iwt} \left[Ae^{iwx/c} - Be^{-iwx/c} \right] \tag{33}$$

$$p(x,t) = iw\rho e^{iwt} \left[Ae^{iwx/c} + Be^{-iwx/c} \right] \tag{34}$$

The two constants A and B are determined by the boundary conditions. These boundary conditions are generally expressed as either the pressure and/or velocity at one or both end points of the pipe or the ratio of the pressure and velocity representing the impedance at that end. Clearly, two of these end conditions are required to define A and B and, thus, to solve eqs. (33) and (34).

To indicate the form of the final solution, assume that $p(o,t) = P_o$ and $v(L,t) = V_L$ are known. Using eqs. (33) and (34)

$$P_o = iw\rho e^{iwt} (A + B)$$

$$V_L = \frac{iwe^{iwt}}{c} (Ae^{iw\tau} - Be^{-iw\tau})$$

where $\tau = L/c$. Solving for A and B,

$$A = \frac{i}{w} e^{-iwt} \left[\frac{-P_o}{\rho} + \left(V_L c + P_o\!\!\Big/\!\rho \ e^{iw\tau} \right)\!\!\left(\frac{1}{e^{iw\tau} + e^{-iw\tau}} \right) \right]$$

$$B = \frac{-ic}{w} e^{-iwt} \left(V_L + \frac{P_o}{\rho c} e^{iw\tau} \right)\!\!\left(\frac{1}{e^{iw\tau} + e^{-iw\tau}} \right).$$

These two values can now be substituted into eqs. (33) and (34), and the velocity and pressure at any other points can be computed. Solving for $p(L,t)$ and $v(o,t)$ yields

$$p(L,t) = 2P_o \frac{e^{-iw\tau}}{1 + e^{-i2w\tau}} - \rho c V_L \left(\frac{1 - e^{-i2w\tau}}{1 + e^{-i2w\tau}} \right) \tag{35}$$

$$v\,(o,t)\;=\;\frac{P_0}{\rho c}\;\;\frac{\left(1 - e^{-i2w\tau}\right)}{\left(1 + e^{-i2w\tau}\right)}\;+\;2V_L\,\frac{e^{-iw\tau}}{1 + e^{-i2w\tau}}\;. \qquad (36)$$

D'Souza and Oldenburger [10] included the effect of viscosity in the
solution for the case of laminar flow. They conclude that the viscosity
effects are characterized by the parameter $\left[a\,(w/\nu)^{1/2}\right]$ where "a" is
the pipe radius, "w" the circular frequency, and "ν" the kinematic
viscosity. As this parameter decreases the viscosity effects increase.
However, the authors do not indicate any critical value of the parameter,
above which the viscosity effects can be neglected. In their tests
$\left[a(w/\nu)^{1/2}\right]_{max} = 36.8$. In the air tests to be run in this study,
which are discussed briefly in the following section, the minimum value
of this parameter is approximately 124. Currently, there is no intention
of considering the viscous effects in the test results obtained in the
present study.

Test Program

The test program for the study of the generation and transmission of acoustic waves and of acoustic damper concepts is established, all the necessary hardware and instrumentation has been ordered, and most of it has arrived. The tests should be initiated by the week of 11 April 1966. This test program is outlined here.

The hot-wire anemometer has arrived at Rocketdyne although the calibrator and temperature compensating probes have not yet arrived. These are not expected to hold up tests, but complete interpretation of the data may be delayed. The suppliers of the Schavitz-Bytrex transducers have delayed delivery but have promised delivery within two weeks.

In connection with the experimental phase of the study of acoustic wave generation, the flow field leaving the impeller blades of an F-1 pump must be determined, and its diffusion through momentum transfer determined as a function of distance from the impeller tip. These tests are to be performed in the F-1 air rig using both 6 and 6+6 vane LOX and fuel pumps and will be accomplished by measuring the flow field with the hot-wire anemometer at various points in the discharge system. Initially, the flow measurements will be made by traversing the discharge flow channel along the dashed lines A-A' in Fig. 7. At each point two probe orientations are required to compute the tangential and radial velocity components illustrated in Fig. 7 where the axial velocity component is assumed to be zero.

Initial tests in the wave transmission study will be conducted in an air system consisting of straight pipes with one or more simple discontinuities (e.g., elbows, tees, orifices, horn, and/or valves) driven by the horn driver. A typical test system is shown in Fig. 8. The components to be tested are given below.

a. Straight pipe. Tests with a straight pipe will be made to verify the one-dimensional time delay solution of the wave equation.

b. Elbows. Ten elbows are required. Three are mitered with turning angles of 30, 60, and 90 degrees, respectively. Six elbows are curved, three with long radii and three with short radii according to commercial designations, with turning angles of 30, 60, and 90 degrees for each radius. The tenth elbow shall be a 90° mitered elbow with turning vanes.

c. Tees. The typical tee joint systems are shown in Fig. 9. Initial tests will be made with open ends. The tees should be of a size that the piping used in the elbow and straight pipe tests can be used.

d. Conical Horn. To test the Mark 10 LOX and fuel valves, a horn is required which expands from the driver diameter to a six inch and then an eight inch diameter. A conical horn is proposed and is shown in Fig. 10. This horn is to be tested with a straight section of 6" or 8" pipe at its discharge. The section of the horn extending from 6" to 8" in diameter is to be slotted for insertion of a removable splitter vane.

ACOUSTIC WAVE GENERATION TEST PROGRAM

MARK 10 LOX OR
FUEL VOLUTE
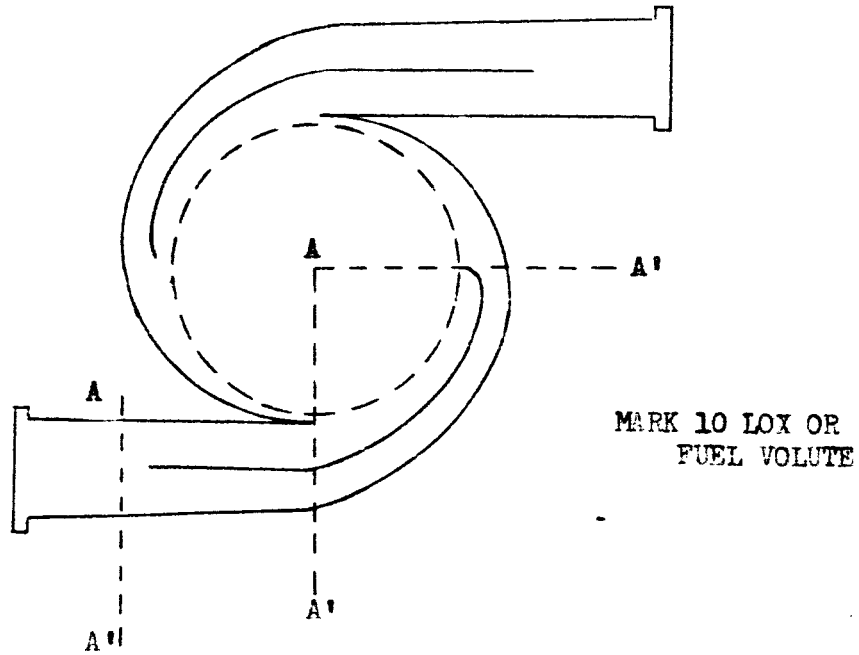
HOT WIRE ANEMOMETER PROBE TO SURVEY FLOW ACROSS THE CHANNEL DEPTH
ALONG THE RADIAL LINES A - A'.

A.

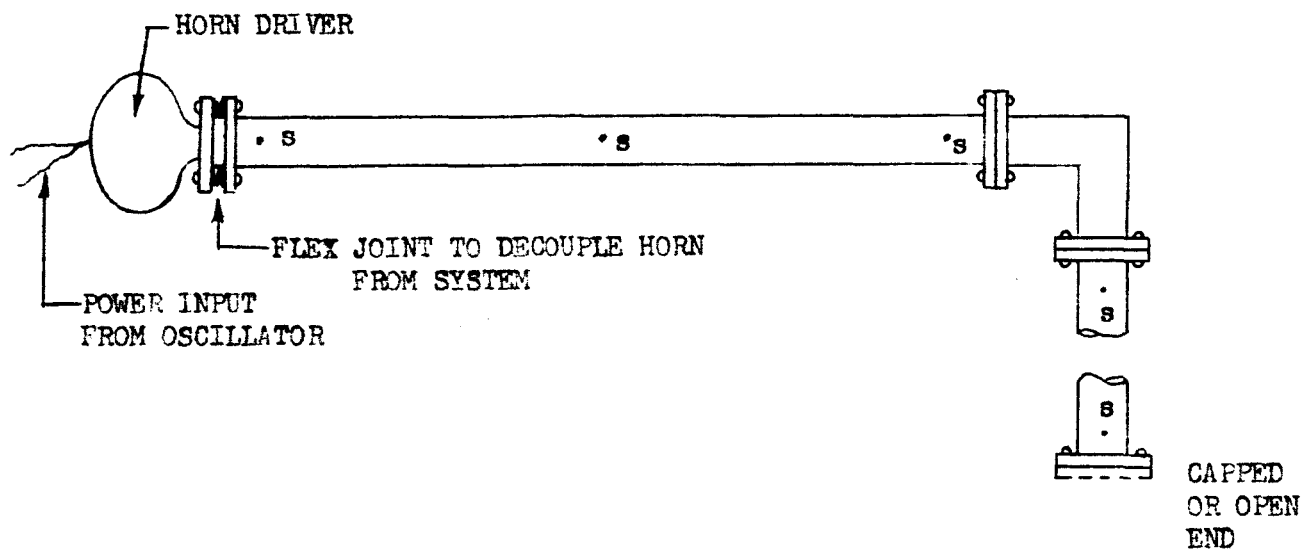B.
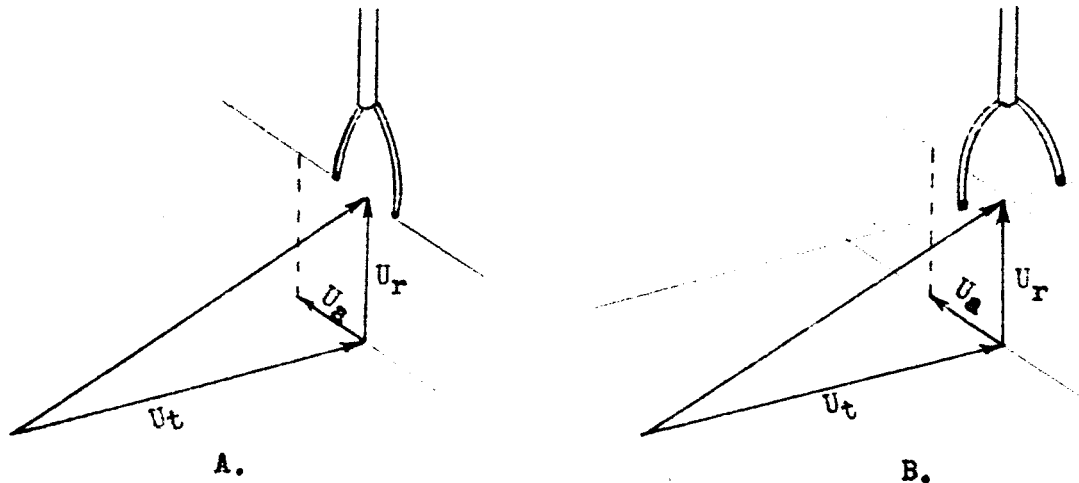
PROBE ORIENTATION

LET U_r = RADIAL FLOW VELOCITY, U_t = TANGENTIAL FLOW VELOCITY,
AND U_a = AXIAL FLOW VELOCITY. IF U_a IS ASSUMED TO BE APPROXIMATELY
ZERO (WHICH IS PROBABLY A GOOD ASSUMPTION IN THE CENTER OF THE
DISCHARGE LINE) THEN ORIENTATION B GIVES U_r ONLY AND ORIENTATION
A GIVES THE VECTOR $\overline{U}_r$ + $\overline{U}_t$.

FIG. 7.

ACOUSTIC WAVE TRANSMISSION TEST PROGRAM

TYPICAL TEST SYSTEM
ACOUSTIC WAVE TRANSMISSION USING HORN DRIVER

s = PRESSURE TRANSDUCER ON ONE SIDE OF DUCT AND HOT WIRE ANEMOMETER PROBE TAP ON OTHER SIDE OF DUCT. (EXACT TAP LOCATIONS TO BE FURNISHED.) TRANSDUCERS ARE KISTLER 606L MODEL.

NOTES:

1. DUCTS MUST BE AT LEAST TEN DIAMETERS LONG.
2. A SOUND ABSORBING UNIT WILL BE SUPPLIED TO THE OPEN END TO MORE ATTAIN A NON-REFLECTING END.
3. HORN DRIVER HAS A 1-3/8" THREADED END. THE DUCT DIAMETER MUST NOT BE MUCH LARGER THAN THIS.
4. THE ENTIRE SYSTEM TO BE SUPPORTED BY SIMPLE MECHANICAL SUPPORTS. MECHANICAL VIBRATIONS ARE NOT EXPECTED TO CREATE A SERIOUS PROBLEM, BUT WEIGHTS MAY BE REQUIRED TO INCREASE THE MASS OF THE SYSTEM.

FIG. 8

TYPICAL TEE JOINT SYSTEMS

OPEN OR
CLOSED END

OPEN OR
CLOSED END

FLEX JOINT

HORN DRIVER

HORN DRIVER

FLEX JOINT

OPEN OR
CLOSED END

OPEN OR
CLOSED END

FIG. 9.

CONICAL HORN

HORN DRIVER AT THIS END

~1.5"

6"

8"

~ 5'

6"   8"

THE SECTION OF THE HORN GOING FROM 6" TO 8" DIAMETER IS TO BE SLOTTED
SUCH THAT A SPLITTER VANE CAN BE ADDED OR REMOVED IN TESTS. WHEN THE
SPLITTER IS REMOVED THE GROOVE INTO WHICH IT FITS MUST BE FILLED TO
GIVE A SMOOTH CIRCULAR INTERNAL CONTOUR.

FIG. 10.

e. Valves. After testing the horn, the Mark 10 LOX and fuel valves will be tested using a system similar to that illustrated in Fig. 8 with the addition of the conical horn at the driver discharge and with the elbow being replaced by the appropriate valve.

f. Orifices. Two sets of orifice tests are to be run using the eight inch pipe sections. The first set of tests will require four orifice plates, each with a single sharp-edged orifice located in its center with orifice to pipe areas of 0.5, 0.1, 0.01, and 0.001, respectively. The second set of tests will have equal total orifice area per test, but the number of orifice holes in the plate will be varied, e.g., with 1, 4, 16, and 64 holes.

Following these component tests the horn driver will be mounted at the tongue of the Mark 10 LOX (and later the fuel) volute in the F-1 air rig. This will permit analysis of the transfer function of the actual volutes. These tests will be followed by tests with the F-1 engine discharge system in place rather than the air rig discharge.

Several acoustic damper concepts described below are to be tested using an air system similar to that shown in Fig. 8, with the horn driver. Each concept is shown in Fig. 11.

1. Tube bundle. A tube bundle of length 1.5 feet and approximately 1.5 inches inside diameter with thin walled tubes 1/4 inch outside diameter shall be tested.

2. Baffles. Using 1/2 closed unsymmetrical orifices a simple baffle system shall be tested. Two baffles are considered sufficient.

3. Screens. Four screens of diameter approximately 1.5 inches and mesh size of 1/8 inch will be tested.

4. Capacitor. A simple capacitor consisting of an enlarged section in the line shall be tested. The diameter ratio proposed is 1/2.

5. Quincke Tube. A Quincke tube splits the oscillation signal into two components then rejoins the components with the phase shift. At the design frequency of the tube, the two components are rejoined exactly out of phase such that they theoretically would cancel each other.

6. Helmholtz Resonator. It is desirable to test a manifold type of Helmholtz resonator, but no specific design has yet been made. The type of resonator under consideration is illustrated in Fig. 11.

I. BLADE WAKE OSCILLATIONS
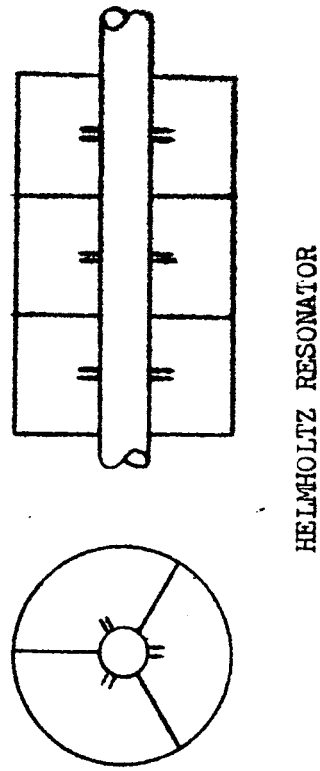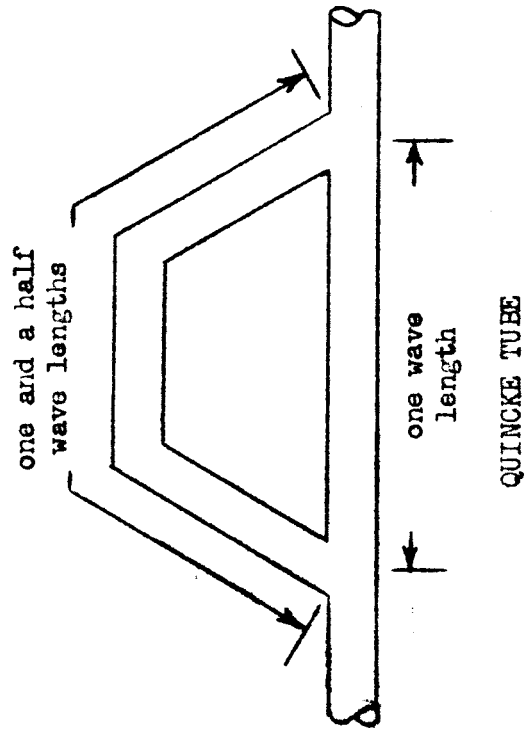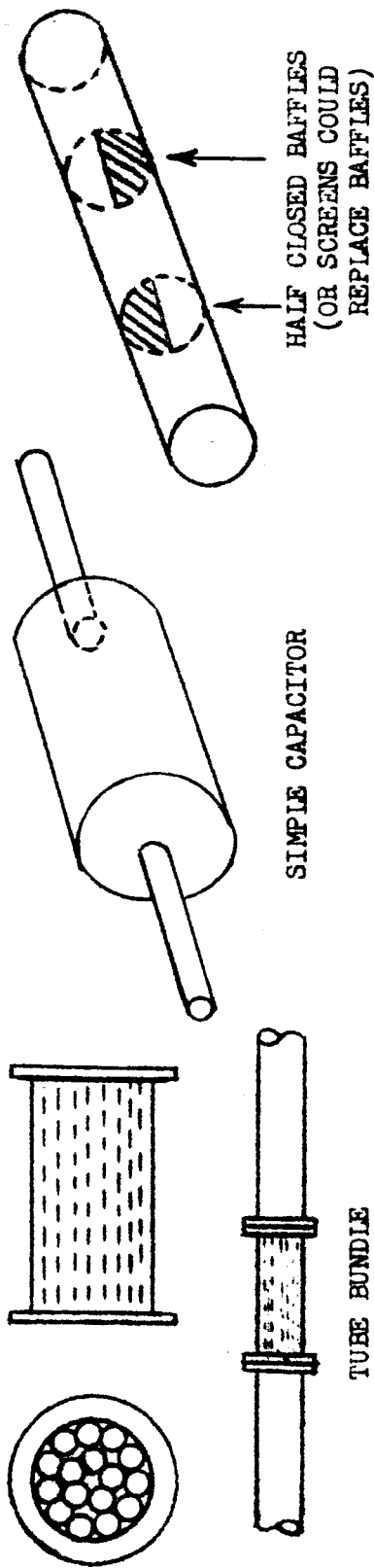
D. ACOUSTIC DAMPER CONCEPTS

HALF CLOSED BAFFLES
(OR SCREENS COULD
REPLACE BAFFLES)

SIMPLE CAPACITOR

TUBE BUNDLE

HELMHOLTZ RESONATOR

one and a half
wave lengths

one wave
length

QUINCKE TUBE

FiG. II.

WAVE REINFORCEMENT

Analytical Development

The relative motion of rotating and stationary parts in a pump is responsible for generating pressure and velocity waves which travel both upstream and downstream of the point of generation. These waves are denoted as acoustic waves since they travel at the acoustic velocity relative to the medium. The acoustic waves of particular concern in turbomachinery are generated as a rotating blade passes a stationary blade, e.g. an impeller blade rotating past a stationary downstream diffuser vane. If there are many such impeller and diffuser vanes, then each time an impeller blade passes any diffuser vane acoustic waves are generated.

If this multi-vaned diffuser feeds a scroll (or volute) with a single discharge and/or inlet, then the waves from each diffuser vane will be traveling towards a common point. If these waves reach this point at the same time they will be superimposed, and for our purposes a linear superposition can be assumed. Clearly, each wave has the same frequency and similar amplitudes, however the phase of each wave depends upon its wavelength and the distance from the point of superposition to the point of origin of the wave. If each wave is exactly in phase wave reinforcement is said to occur, and the resulting wave amplitude will,with our approximations, be simply the sum of the amplitude of each of the individual waves. For example, with 20 diffuser vanes wave reinforcement due to phase coincidence would result in a discharge wave amplitude 20 times the amplitude generated at each vane. If, using again the example case of a 20 vane diffuser, the phase shift of waves from two adjacent vanes is $2\pi/20$ radians, then the vector sum of the 20 amplitudes would result in zero net amplitude. Strub (11) has derived an analytical solution for calculating the pump operating conditions at which wave reinforcement would occur. This solution is presented below.

Consider the case illustrated in Fig. 12 (a) noting particularly the direction of rotation of the impeller. Since only the relative phase of successive waves is of concern, the waves can be assumed to be generated when the impeller,diffuser vanes are in positions corresponding to vanes 1 and E, respectively. It can further be assumed that the time required for a wave to travel from E to C is equal to that from B to D. Therefore, if the wave from E is to be exactly in phase with the wave from B, then the wave from E must travel the distance CD in exactly the time required for the impeller blade 2 to travel from A to B. These conditions can be stated mathematically resulting in Strub's equation for wave reinforcement. (Note that the assumption that the waves travel along such paths as E-C-D is an approximation. However, since adjacent diffuser sections are generally geometrically similar and since only the relative phase of adjacent waves is of interest, this assumption will not introduce any significant error.)
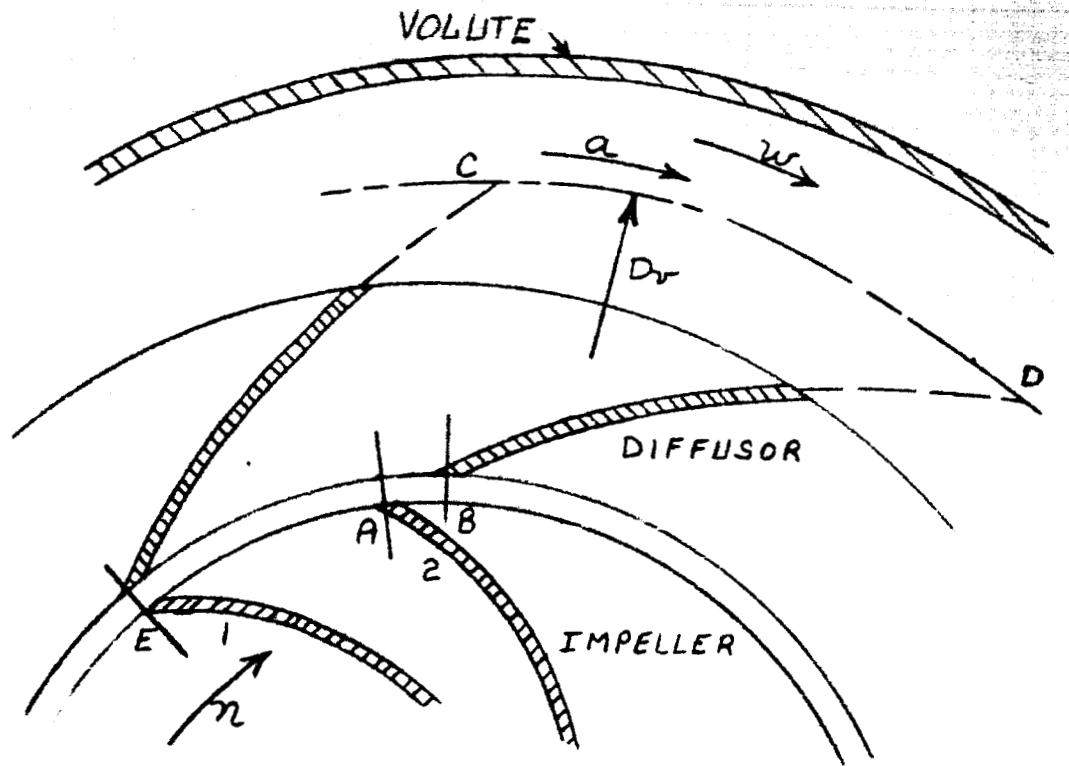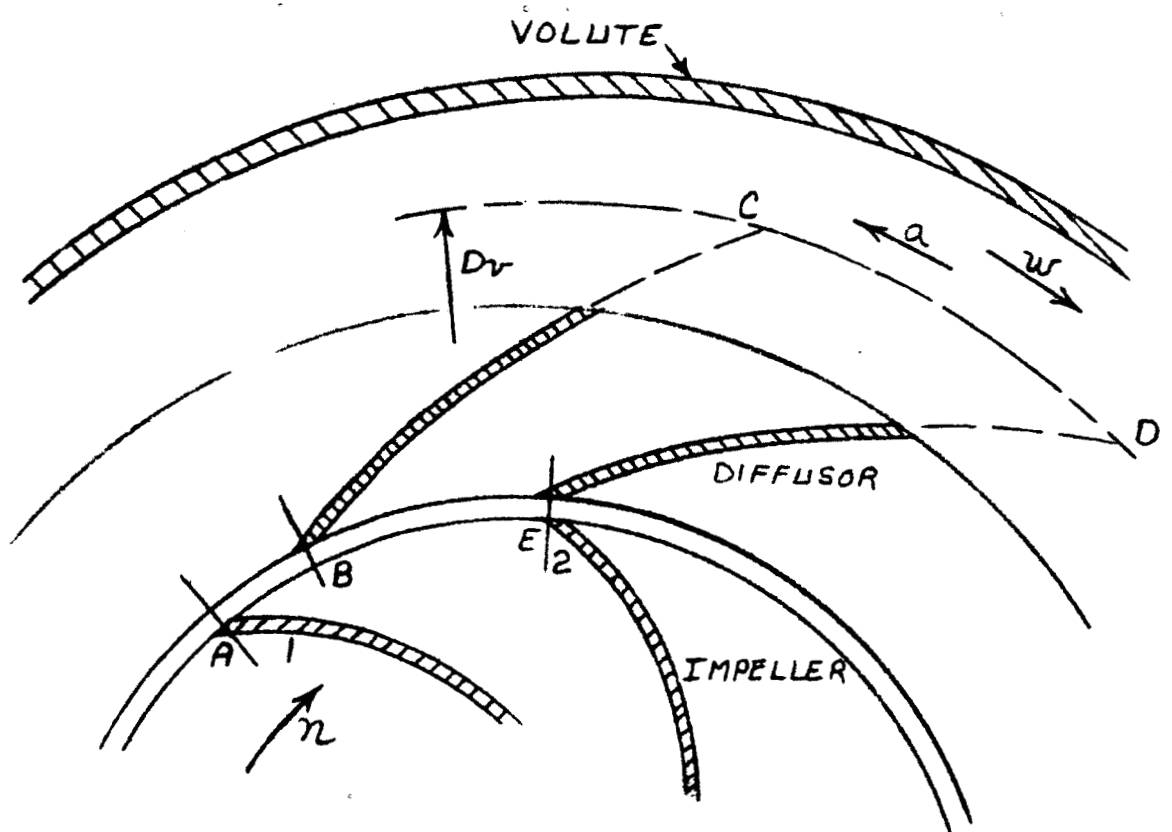
FIGURE 12 a.

FIGURE 12 b.

The spacing of the impeller vanes is given by

$$\overline{EA} = \pi D_i / Z_i \tag{37}$$

where D_i is the impeller outer diameter (o.d.) and Z_i is the number of impeller vanes. The spacing between the diffuser vanes projected along the impeller o.d. is

$$\overline{EB} = \pi D_i / Z_d \tag{38}$$

where Z_d is the diffuser vane number. Therefore, the distance $\overline{AB}$ is

$$\overline{AB} = \pi D_i \left(\frac{1}{Z_d} - \frac{1}{Z_i} \right). \tag{39}$$

The velocity of the impeller at its o.d. is

$$V_i = \pi D_i n \tag{40}$$

where n is the pump rotational speed in rps. Thus, the time required for impeller vane #2 to travel from A to B is

$$t_1 = \overline{AB} / V_i = \frac{1}{n} \left(\frac{1}{Z_d} - \frac{1}{Z_i} \right). \tag{41}$$

With an oscillation frequency given as $jZ_i n$ (where j is the order of the harmonic, $j = 1$ being the fundamental impeller blade frequency), the number of pressure oscillations in time t_1 is

$$\theta_1 = f t_1 = \left(\frac{1}{Z_d} - \frac{1}{Z_i} \right) jZ_i \tag{42}$$

Letting D_v equal the mean volute diameter

$$\overline{CD} = \pi D_v / Z_d \tag{43}$$

The wave velocity along $\overline{CD}$ is

$$V_w = a + w \qquad (44)$$

where a is the acoustic velocity of the medium and w is the mean velocity in the volute. The time required for a wave to travel the distance $\overline{CD}$ is

$$t_2 = \frac{\pi D_v}{Z_d (a + w)} \ . \qquad (45)$$

Therefore, the number of oscillations in the length $\overline{CD}$ is

$$\theta_2 = \frac{\pi D_v \, jZ_i n}{Z_d (a + w)} \ . \qquad (46)$$

The criterion for phase coincidence of two adjacent waves is that the difference between the number of oscillations along CD and the number of oscillations generated in the time required for the impeller to travel the distance AB be a whole number, or

$$\theta_1 - \theta_2 = m \ . \qquad (47)$$

Substituting eqs. (42) and (46) into eq. (47) and solving for m/j yields

$$\frac{m}{j} = \frac{Z_i}{Z_d} \left[\frac{Z_d - Z_i}{Z_i} + \frac{\pi D_v n}{a + w} \right] \ . \qquad (48)$$

The average velocity in the volute collector scroll is approximately a constant and can be determined from the flow rate and area at the volute discharge. With Q = volumetric flow rate in gpm and A = discharge area in square inches

$$w = \frac{0.321 \, Q}{A} \ .$$

Or, in terms of the flow coefficient

$$w = \frac{0.321 \ (Q/N) \ (60 \ n)}{A}$$

$$w = \frac{19.26 \ (Q/N) \ n}{A} \tag{49}$$

where the pump speed is given by N in rpm and n in rps as before.

Substituting eq. (49) into eq. (48), and solving for pump speed yields

$$N = 60n = 60.0 \ \frac{a \left[1 + Z_d/Z_i \ (m/j - 1 \ ) \right]}{\pi D_v - \frac{19.26}{A} \left(\frac{Q}{N} \right) \left[1 + \frac{Z_d \ (m/j \ -1)}{Z_i} \right]} . \tag{50}$$

This equation permits computation of the speeds at which a given harmonic will result in wave reinforcement. There are two significant characteristics of eq. (50) which should be mentioned. First, to scale the results for various fluids requires only a ratio of the acoustic velocities of the fluid. Secondly, the conditions for wave reinforcement do not depend on the spacing between the impeller and diffuser vanes.

Following the same procedure the criterion for phase coincidence at the beginning of the volute can be developed for the case presented in Fig. 12b. In this case the number of oscillations generated in the time required for the impeller to travel the distance AB is

$$\Theta_1 = \left[\frac{1}{Z_i} - \frac{1}{Z_d} \right] j \ Z_i . \tag{51}$$

The velocity of propagation of the waves along $\overline{CD}$ is now $(a - w)$ such that the number of oscillations along CD is

$$\Theta_2 = \frac{\pi D_v \ j Z_i \ n}{Z_d \ (a - w)} . \tag{52}$$

Substituting into eq. (47) and solving for m/j

$$\frac{m}{j} = \frac{Z_i}{Z_d} \left[\frac{Z_d - Z_i}{Z_i} - \frac{\pi D_v n}{(a - w)} \right] \tag{53}$$

Solving now for pump speed using eq. (49)

$$N = -60.0 \, a \frac{\left[1 + \dfrac{Z_d}{Z_i} \left(\dfrac{m}{j} - 1\right)\right]}{\pi D_v - \dfrac{19.26 \ (Q/N)}{A} \left[1 + \dfrac{Z_d}{Z_i} \left(\dfrac{m}{j} - 1\right)\right]} \qquad (54)$$

Numerical Calculations

Several Rocketdyne pumps with multi-vaned diffusers were analyzed for determining the speeds at which wave reinforcement would occur, i.e. the Mark 3, Mark 19, and Mark 26 fuel pumps. The Mark 3 and Mark 19 fuel pumps each have 13 diffuser vanes, but the Mark 3 pump has 10 impeller vanes while the Mark 19 pump has 24 impeller vanes. Thus, these two pumps each represent one of the two cases of the impeller vane number being greater or less than the diffuser vane number.

The points at which wave reinforcement would occur was determined by plotting pump speed versus the parameter (m/j) as given by eq. (50) or (54). The resulting curve is shown for the Mark 3, Mark 19, and Mark 26 pumps in Figs. 13, 14, and 15, respectively, in each case using the data presented with the curve. In all cases the fluid is air. The points at which wave reinforcement occurs are shown for the first three harmonics. In general, each successive harmonic is expected to be much less in amplitude than the preceding one such that only the first two or three are of interest. Note that at many points more than one harmonic will reinforce, e.g. at $m = 0$, all harmonics are reinforced.

The Mark 26 pump is being built up for testing in the J-2 air rig. The tests will cover the range from 3000 to 10,000 rpm such that the point, $m/j = 0$, will be included in the tests. By filtering the data the amplitudes of the various harmonics can be determined.

In testing any of the above pumps in air, the discharge pressures and temperatures do not change significantly with pump speed. As a result, the acoustic velocity can be maintained as a constant for all speeds. However, if the curves were to be plotted using the fuel as the fluid, the change in discharge pressures and temperatures due to changes in pump speed would result in significant changes in the acoustic velocity. Furthermore, the discharge pressure and temperature are not just a function of speed. Thus, the actual operating conditions are required to determine accurately the acoustic velocity and the conditions of wave reinforcement. This would complicate efforts to scale the results from one fluid to another over a very large speed range.

MARK 3 FUEL PUMP
WAVE REINFORCEMENT AT THE VOLUTE INLET

IMPELLER BLADE NUMBER = 10
DIFFUSER VANE NUMBER = 13
VOLUTE DISCHARGE AREA = 1.43"
MEAN VOLUTE DIAMETER = 18"
OPERATING Q/N = 0.302
FLUID = AIR

REINFORCEMENT OF THE jTH
HARMONIC OCCURS WHEN m IS
ANY INTEGER.

PUMP SPEED - RPM X 10^{-3}

PARAMETER m/j
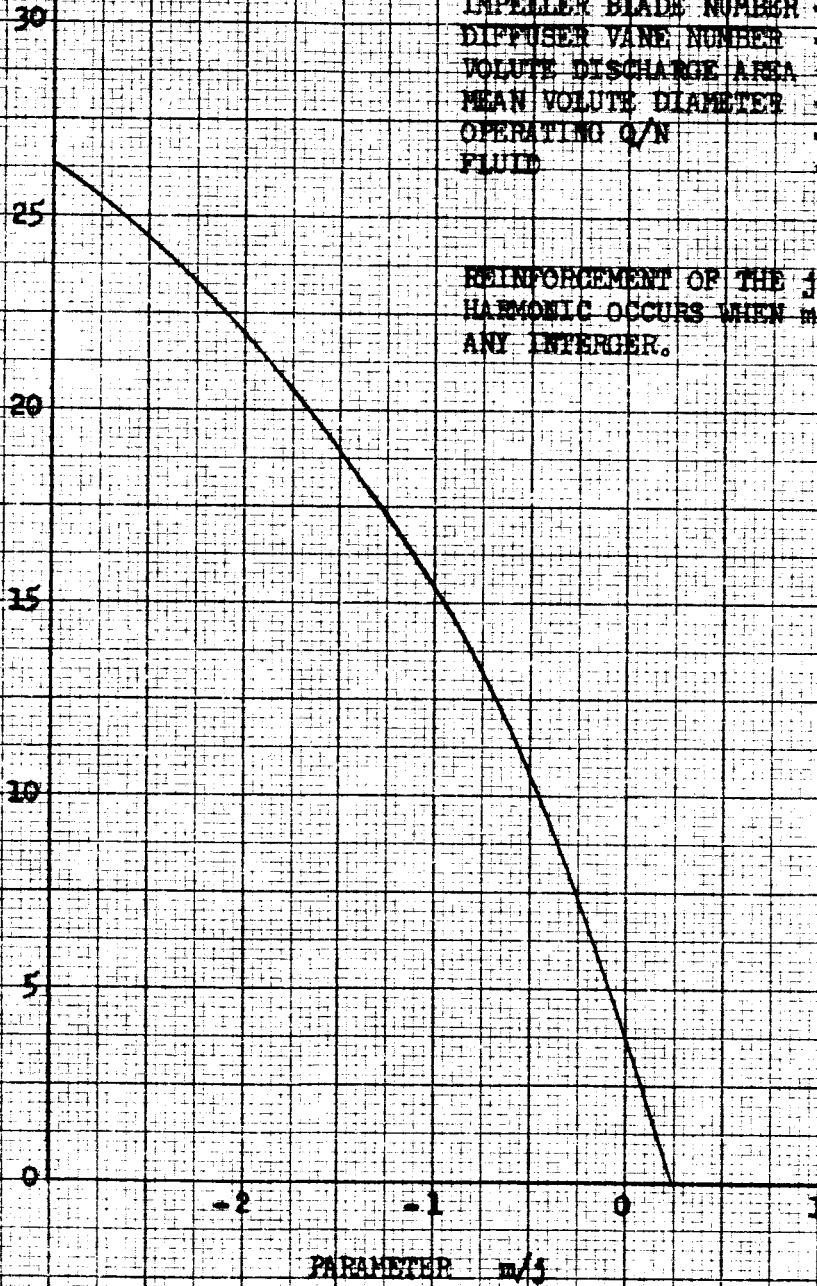
POINTS OF
REINFORCEMENT:

HARMONIC: 2 $\frac{1}{2}$ 2 $\frac{1}{2}$ 2 $\frac{1}{2}$ 2 $\frac{1}{2}$
          3   3   3   3   3   3   3   3   3   3   3

FIG. 13.

MARK 19 FUEL PUMP
WAVE REINFORCEMENT AT THE VOLUTE DISCHARGE

IMPELLER BLADE NUMBER = 24
DIFFUSER VANE NUMBER = 13
VOLUTE DISCHARGE AREA = 2.37"
MEAN VOLUTE DIAMETER = 14.4"
OPERATING Q/N = 0.138
FLUID = AIR

REINFORCEMENT OF THE jTH
HARMONIC OCCURS WHEN m IS
ANY INTEGER.

FIG. 14.

MARK 26 FUEL PUMP
WAVE REINFORCEMENT AT THE VOLUTE DISCHARGE

IMPELLER BLADE NUMBER = 29
DIFFUSER VANE NUMBER = 19
VOLUTE DISCHARGE AREA = 12.56"
MEAN VOLUTE DIAMETER = 12.20"
OPERATING Q/N = 0.398
FLUID = AIR

REINFORCEMENT OF THE JTH
HARMONIC OCCURS WHEN m IS
ANY INTEGER.

PUMP SPEED - RPM N·10⁻³
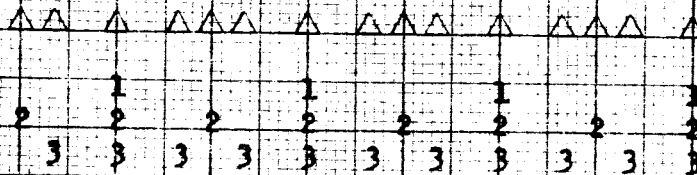
PARAMETER m/j

POINTS OF REINFORCEMENT

HARMONIC

FIG. 15.

CAVITATION INDUCED OSCILLATIONS

A digital computer program has been developed which will yield the theoretical cavity volume for any inducer as a function of the incidence angle and the cavitation number. This information must now be put into a form suitable for determining if this cavity volume will indicate the frequency and/or amplitude of the cavitation induced oscillations. The cavity volume relationships can be modeled on the analog computer for oscillation analysis purposes. If dynamic pressure and flow data were available at the inlet and discharge of an inducer the cavity theory could be evaluated. However, since flow data is not available, the complete test system in which the dynamic pressure data was obtained must be modeled on the analog computer also. Since the purpose of this model is to verify the concepts and results established concerning the cavity volume, then the model of the rest of the system must be as accurate as is possible. Since the dynamic properties of an impeller are unknown. a model of any pump test facility would not contain the accuracy required for verifying the inducer performance. As a result the Rocketdyne water tunnel system used for testing inducers alone must be modeled.

A schematic diagram of the water tunnel is shown in Fig. 16. Since interest is only in low frequency oscillations (f $\leq$ 50 cps), complexities such as elbows, diffuser sections, etc. will in general not affect the transmission of waves and can be ignored. However, since these oscillations occur at low values of NPSH, cavitation in the system at points other than at the inducer becomes more probable. To determine the effects of the inducer cavity volume any other cavity volume in the system must be accounted for in the system model. In the water tunnel system cavitation is believed to occur at some of the mitered elbows and possibly elsewhere in the system. To account for this, dynamic pressure data would have to be obtained at intermediate points throughout the system as shown in Fig. 16. All existing dynamic data has been obtained with pressure transducers at the locations P-1 and P-2 only. Cost estimates were obtained for installing the other transducers noted in the figure and for running a short test program even though these items were not included in the original proposal. However, the costs were larger than could be diverted to this effort during the current program. Thus, the system will be modeled under the assumption of no cavitation other than at the inducer. The results obtained from the analog computer study should at least indicate the desirability of pursuing this approach in which case this test program would be required.
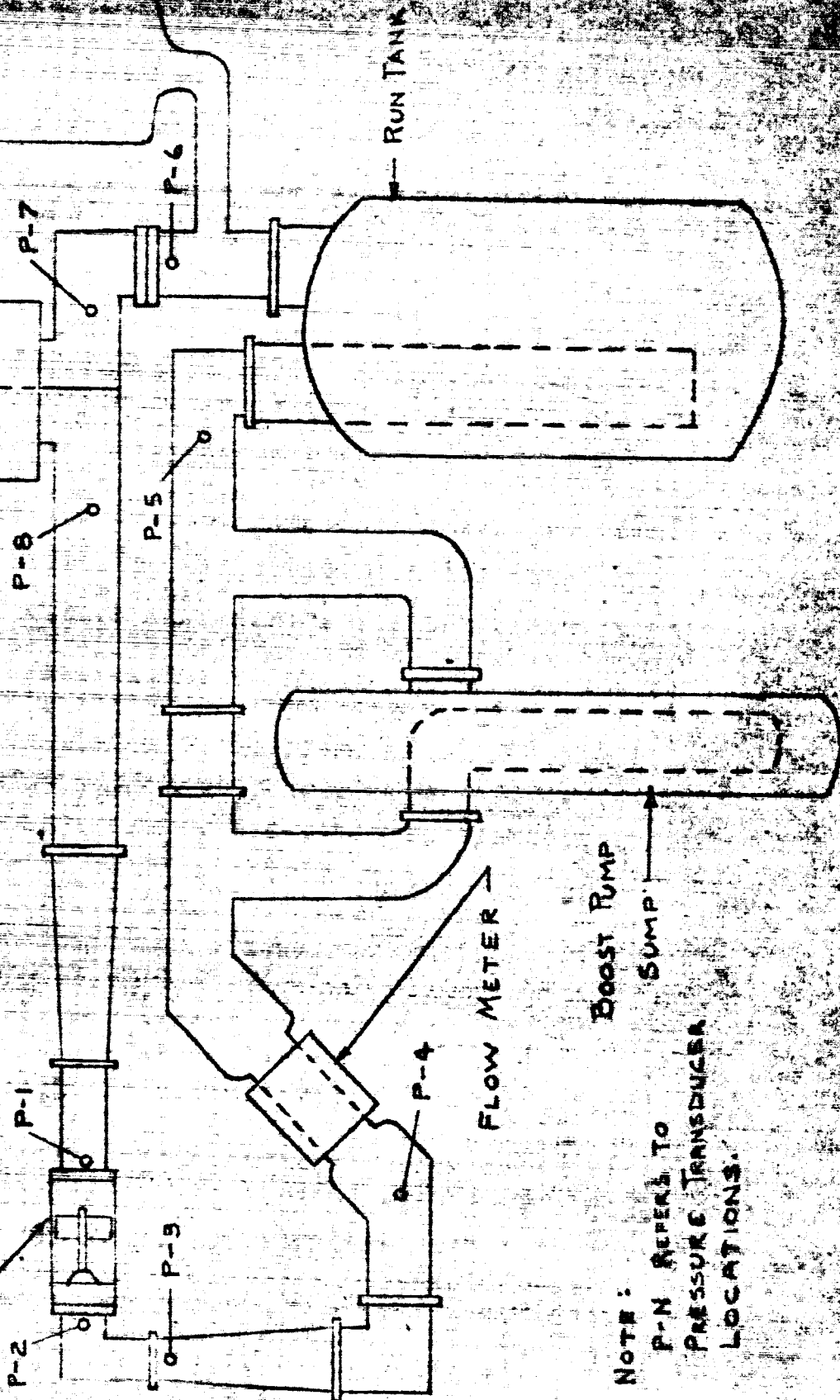
Currently, measurements of the water tunnel system are being obtained after which the system will be modeled on the computer.

CTL-1 WATER TUNNEL

VIEWING SECTION

PRESSURE Co.

FILTER

RUN TANK

FLOW METER

BOOST PUMP

SUMP

P-1
P-2
P-3
P-4
P-5
P-6
P-7
P-8

T4

NOTE:
P-N REFERS TO
PRESSURE TRANSDUCER
LOCATIONS.

FIG 16.

PROGRAM SCHEDULE

A time extension of two months has been requested by Rocketdyne as a result
of the three month delay in testing due to problems encountered with the
hot-wire anemometer. Assuming this extension will be granted, the schedule
planned for completing the current study program is shown in Fig. 17. As
has been discussed and verbally agreed upon by NASA the effort on the stall
oscillation analysis is of lowest priority and has been scheduled at the end
of the program. This analysis will be completed only as time and costs permit.

PUMP DISCHARGE PRESSURE OSCILLATIONS STUDY

SCHEDULE* FOR PROGRAM COMPLETION

TASKS AND SUBTASKS	APRIL	MAY	JUNE	JULY	AUGUST
I. BLADE WAKE OSCILLATIONS					
A. Acoustic Wave Generation					
Tests and data analysis					
B. Acoustic Wave Transmission					
1. Component tests					
2. System analysis					
3. System tests					
C. Wave Reinforcement					
Tests and data analysis					
D. Acoustic Dampers					
1. Analysis					
2. Tests					
II. CAVITATION INDUCED OSCILLATIONS					
1. Analog computer study					
2. Related analysis					
III. STALL OSCILLATIONS					
1. Analysis					
2. Test data analysis					
IV. REPORTS					
1. Monthly or Quarterly					
2. Final					

*Schedule assumes two month time extension on program.

FIGURE 17

REFERENCES

1. Th. Von Karman and W. R. Sears, "Airfoil Theory for Non-Uniform Motion", Journal of the Aeronautical Sciences, Vol. 5, No. 10, Aug. 1938, pp. 379-390.

2. N. H. Kemp and W. R. Sears, "The Unsteady Forces Due To Viscous Wakes In Turbomachines", Journal of the Aeronautical Sciences, Vol. 22, No. 7, 1955, pp. 478-483.

3. N. H. Kemp and W. R. Sears, "Aerodynamic Interference Between Moving Blade Rows", Journal of the Aeronautical Sciences, Vol. 20, No. 9, 1953, pp. 585-597.

4. R. X. Meyer, Interference Due To Viscous Wakes Between Stationary and Rotating Blades In Turbomachines, Doctor of Engineering Thesis, The John Hopkins University, 1955.

5. M. D. Lefcort, "An Investigation Into Unsteady Blade Forces In Turbomachines", A.S.M.E. Transactions, Paper No. 64-WA/GTP-3.

6. L. J. Sivian, "Acoustic Impedance of Small Orifices", Journal of the Acoustic Society of America, Vol. 7, Oct. 1935, pp. 94-101.

7. L. E. Kinsler and A. R. Frey, Fundamentals of Acoustics, John Wiley and Sons, Inc., New York, 1950.

8. D. H. Utvik, A. W. Blackman, and H. J. Ford, "Evaluation of Absorption Liners for Suppression of Combustion Instability In Rocket Engines", American Institute of Aeronautics and Astronautics, Paper No. 65-585, AIAA Propulsion Joint Specialist Conference, Colorado Springs, Colo., June 1965.

9. R. H. Bolt, S. Labate, and U. Ingard, "The Acoustic Reactance of Small Circular Orifices", Journal of the Acoustic Society of America, Vol. 21, No. 2, 1949, pp. 94-97.

10. A. F. D'Souza and R. Oldenburger, "Dynamic Response of Fluid Lines", A.S.M.E. Transactions, Paper No. 63-WA-73.

11. R. A. Strub, "Pressure Fluctuations and Fatigue Stresses In Storage Pumps and Pump-Turbines", A.S.M.E. Transactions, Paper No. 63-AHGT-11.